MT1 and MT2 melatonin receptors play opposite roles in brain cancer progression

MT1 and MT2 melatonin receptors play opposite roles in brain cancer progression

Kinker GS[1#], Ostrowski LH[1], Ribeiro PAC[2], Chanoch R[3], Muxel SM[1], Tirosh I[3], Spadoni G[4], Rivara S[5], Martins VR[2,6], Santos TG[2,6], Markus RP[1], Fernandes PACM[1#].

[1]Dep. of Physiology, Institute of Bioscience, University of Sao Paulo, Sao Paulo, Brazil.

[2]International Research Center, A.C. Camargo Cancer Center, Sao Paulo, Brazil.

[3]Dep. of Molecular Cell Biology, Weizmann Institute, Israel.

[4]Dep. of Biomolecular Sciences, University of Urbino "Carlo Bo", Urbino, Italy

[5]Dep. of Food and Drug, University of Parma, Parma, Italy.

[6]National Institute for Science and Technology in Oncogenomics and Therapeutic Innovation – INCITO-INOTE.

Corresponding authors: gabriela.kinker@gmail.com / pacmf@usp.br

Keywords: Glioma, medulloblastoma, MT1, MT2, MTNR1A, MTNR1B

Abstract

Primary brain tumors remain among the deadliest of all cancers. Glioma grade IV (glioblastoma), the most common and malignant type of brain cancer, is associated with a 5-year survival rate < 5%. Melatonin has been widely reported as an anticancer molecule and we have recently demonstrated that the ability of gliomas to synthesize and accumulate this indolamine in the surrounding microenvironment negatively correlates with tumor malignancy. However, our understanding of the specific effects mediated through the activation of melatonin membrane receptors remains limited. Thus, here we investigated the specific roles of MT1 and MT2 in gliomas and medulloblastomas. Using the MT2 antagonist DH97, we showed that MT1 activation has a negative impact on the proliferation of human glioma and medulloblastoma cell lines, while MT2 activation has an opposite effect. Accordingly, gliomas have a decreased mRNA expression of *MT1* (also known as *MTNR1A*) and an increased mRNA expression of *MT2* (also known as *MTNR1B*) compared to the normal brain cortex. The MT1/MT2 expression ratio negatively correlates with the expression of cell cycle-related genes and is a positive prognostic factor in gliomas. Notably, we showed that functional selective drugs that simultaneously activate MT1 and inhibit MT2 exert robust anti-tumor effects *in vitro* and *in vivo*, downregulating the expression of cell cycle and energy metabolism genes in glioma stem-like cells. Overall, we provided the first evidence regarding the differential roles of MT1 and MT2 in brain tumor progression, highlighting their relevance as druggable targets.

Introduction

Despite decades of research progress, brain tumors remain among the cancers that hold the poorest prognosis. Glioma grade IV (glioblastoma), the most common and malignant type of brain cancer, is associated with a median survival of approximately 15 months in adults[1,2]. Challenges in the treatment of such tumors include their invasive nature and cellular heterogeneity, as well as the difficulty of drug delivery across the blood-brain barrier[3]. In 2016, the World Health Organization has incorporated biologically and clinically relevant molecular features to the traditional histological classification of central nervous system tumors[4,5]. Diffuse gliomas in adults are now divided into three main groups with progressively worse prognosis: isocitrate dehydrogenase (IDH)-mutant and 1p/19q co-deleted tumors with oligodendroglial morphology; IDH-mutant and non-1p/19q co-deleted tumors with astrocytic morphology; and IDH-wild type glioblastomas. New entities also include diffuse midline pediatric glioma with H3 K27M–mutations, RELA fusion–positive ependymoma, medulloblastoma WNT-activated, and medulloblastoma SHH-activated[4,5].

Melatonin synthesized by the pineal gland at night translates the environmental dark phase to the organism and ensures the synchronization of circadian and seasonal rhythms[6,7]. The production of melatonin has also been detected in many extrapineal tissues, including the retina[8], gastrointestinal tract[9], bone marrow[10,11] and brain[12,13]. Generally, extrapineal melatonin exerts local autocrine and paracrine effects[13–15], acting through biological mechanisms such as activating G protein-coupled receptors and directly scavenging of free radicals[16]. Human MT1 and MT2 melatonin receptors share 55% of amino acid sequence similarity and bind melatonin with high affinity[17]. Both are typically coupled to Gi/o proteins, while MT1 can also be couple to Gq, evoking phospholipase-c calcium-dependent signaling[18,19]. Melatonin receptors are widely expressed throughout the central nervous system[20] and play a role in circadian entrainment, synaptic function and neurodevelopment[21]. Interestingly, altered expression of melatonin receptors has been reported in different neurodegenerative conditions such as Alzheimer's and Parkinson's diseases[22–24].

Melatonin is increasingly recognized as an antitumor molecule across a wide variety of malignancies[25,26]. Accordingly, we have demonstrated that the ability of gliomas to synthesize and accumulate melatonin negatively correlates with their overall malignancy [12]. High-grade gliomas

have a decreased expression of acetylserotonin O-methyltransferase (*ASMT*), the final enzyme of melatonin biosynthesis, combined with a high expression of cytochrome P450 1B1 (*CYP1B1*), the main enzyme of melatonin extra-hepatic metabolism. Importantly, the content of melatonin in the tumor microenvironment, as predicted by the ASMT:CYP1B1 expression index, was a positive prognostic factor, independent of glioma grade and histological subtype[12]. Additionally, high concentrations of melatonin (mM range) have been shown to impair the invasion and migration of human glioma cell lines and reduce the viability of glioma-initiating cells, while lower concentrations did not produced significant results[27–29]. MT1 and MT2 bind melatonin with nM affinity[19], thus effects observed only at the mM range likely involve receptor-independent mechanisms.

Few studies have assessed the role of MT1 in brain cancer, while no data is available regarding MT2. In glioma stem cells, MT1 activation has been shown to inhibit the expression of nestin, p-c-Myc(S62), and c-Myc, suppressing neurosphere formation and inducing G2/M arrest[30]. Moreover, in gliomas with increased expression of MT1, melatonin treatment exerts a more pronounced impairment of cell growth both *in vitro* and *in vivo*[31]. Thus, despite previous efforts, the relevance of melatonin receptors as potential targets for the treatment of brain cancer remains largely unexplored. To provide a framework for the rational use of melatonin and other melatonergic compounds in brain cancer therapy, here we dissected the differential impacts of MT1 and MT2 activation in human gliomas a medulloblastomas. Using a MT2-selective antagonist we revealed that MT1 impairs, while MT2 promotes, the proliferation of glioma and medulloblastoma cell lines. Accordingly, patients expressing high *MT1* (also known as *MTNR1A*) and low *MT2* (also known as *MTNR1B*) presented less aggressive tumors and significantly better prognosis. Finally, we show that functional selective drugs displaying MT1 agonist and MT2 antagonist properties exert robust anti-tumor effects *in vivo* and *in vitro*, and interfere with the proliferation and metabolism of glioma stem cells.

Materials and methods

Cell lines

Human glioma cell lines HOG, T98G, U87MG, U87MG-luc (expressing a luciferase reporter gene), and human medulloblastoma cell line DAOY were cultured in RPMI 1640 medium (Thermo Fisher Scientific) supplemented with 10% heat-inactivated fetal bovine serum (Thermo Fisher Scientific), 100 IU/mL penicillin (Thermo Fisher Scientific), and 100 μg/mL streptomycin (Thermo Fisher Scientific). T98G, U87MG and DAOY were purchased from ATCC, HOG was kindly provided by Dr. Suely K. N. Marie (University of Sao Paulo, Sao Paulo, Brazil), and U87MG-luc was kindly provided by Dr. Andrew L. Kung (Memorial Sloan Kettering Cancer Center, New York, USA). Cancer stem cell-enriched cultures MGG23 and MGH143 were derived from glioblastoma specimens at the Massachusetts General Hospital and kindly provided by Dr. Mario Suvà (Dana-Farber Cancer Institute, USA). MGG23 and MGH143 cells were grown as neurospheres and maintained in neurobasal medium (Thermo Fisher Scientific) supplemented with L-glutamine (Thermo Fisher Scientific), B27 supplement (Thermo Fisher Scientific), N2 supplement (Thermo Fisher Scientific), 100 IU/mL penicillin (Thermo Fisher Scientific), 100 μg/mL streptomycin (Thermo Fisher Scientific), 20 ng/mL EGF (Sigma), and 20 ng/mL FGF2 (Peprotec). All cell lines were cultured at 37°C in a humidified atmosphere of 5% CO_2.

Flow cytometry

Cells were detached with 0.2% EDTA (10 min, room temperature), fixed with 2% PFA PBS (20 min, on ice), permeabilized with 0.1% TritonX-100 PBS (10 min, room temperature), blocked with 2% BSA PBS (1h, room temperature) and incubated overnight at 4°C with goat anti-MT1 (1:100, sc-13186, Santa Cruz Biotechnology) or goat anti-MT2 (1:100, sc-13177, Santa Cruz Biotechnology) primary antibodies. Cells were washed twice with 2% BSA PBS before incubation with FITC-conjugated anti-goat IgG secondary antibody (1:200, sc-2777, Santa Cruz Biotechnology) for 1 h at room temperature. Cells stained with the secondary antibody alone were used as the isotype control. Data were acquired on an Amnis FlowSight flow cytometer (Merck Millipore) and analyses were carried on using the IDEAS software (Merck Millipore) and FlowJo v9.

MTT proliferation assay

Cells (4 x 10^3 per well) were seeded on 96-well plates, left to attach overnight and treated with DH97 (3 x 10^{-10} – 10^{-6} M), 5-HEAT (10^{-9} – 10^{-6} M), UCM799 (10^{-9} – 10^{-6} M), or the appropriate vehicle for 48 h. Culture media was then replaced with a MTT solution (0.5 mg/mL in PBS, Sigma) and cells were maintained in the incubator for 4 hr. Reduced MTT crystals (formazan) were dissolved in isopropanol:DMSO (1v:1v) for 10 minutes at room temperature. Absorbance was measured at 570 nm, with background subtraction at 690 nm, in a SpectraMax 250 spectrophotometer (Molecular Devices).

U87MG-luc orthotopic xenograft model

U87MG-luc cells (5×10^5) suspended in 5 µL PBS were injected into the right striatum of female/male 8–10-week-old Balb/C nude mice (Charles River International) using a 10 µL Hamilton syringe attached to a Harvard 22 syringe pump (Harvard Apparatus), as previously describe [32,33]. Two weeks after tumor implantation, animals were randomly assigned to four experimental groups: vehicle (0.2% DMSO, n = 7), 10^{-4} M melatonin (n = 5), 10^{-4} M 5-HEAT (n = 5) and 10^{-4} M UCM799 (n = 5). Treatments were continuously infused (0.25 µl/hr) into the right striatum of mice for 14 days using ALZET mini osmotic pumps (model 1002) and the ALZET brain infusion kit 3 (DURECT Corporation). Prior to implantation, pre-filled pumps were primed in sterile 0.9% saline overnight at 37°C, according to manufacturer's instructions. Given the pump infusion rate, r = 0.25 µl/h, and the average volume (v = 35 µL) and production rate (p = 18 µL/h) of cerebrospinal fluid in mice[34], the expected equilibrium concentration of compounds in the tumor microenvironment is approximately 10^{-6} M, which corresponds to the concentrations of 5-HEAT and UCM799 that exerted maximal inhibition in the *in vitro* dose-response assays (**Fig. 3A-B**).

For *in vivo* bioluminescence imaging, animals were anesthetized with isoflurane, injected intraperitoneally with D-luciferin (50 µg/g, PerkinElmer) and placed into an *In Vivo* FX PRO imaging system (Bruker). Analyses were performed using the MI Software (Bruker). Fourteen days post-treatment, mice were euthanized by deep anesthesia and encapsulated tumors were resected. Tumor volume (mm^3) was determined using width (a) and length (b) measurements ($V = (a^2 \times b)/2$, where $a \leq b$).

Institutional guidelines for animal welfare and experimental conduct were followed. The study was approved by the Animal Ethics Committee of the A. C. Camargo Cancer Center (ID 076/17), and by the Animal Ethics Committee of the Institute of Bioscience, University of Sao Paulo (ID 284/2017).

TCGA and GTEx data

The Cancer Genome Atlas (TCGA) RNA-seq and clinical data from 662 primary gliomas (509 lower grade gliomas and 153 glioblastomas) and Genotype-Tissue Expression (GTEx) RNA-seq data from 283 normal brain cortex were downloaded from the UCSC XENA Browser [35]. RNA-seq data were generated using the Illumina HiSeq 2000 RNA sequencing platform and quantified with RSEM. Estimated counts were upper quartile normalized, $\log_2(normalized\ counts + 1)$ transformed. Expression levels of *MT1* and *MT2* were converted to z-score for calculating the MT1/MT2 expression ratio.

Survival analysis

We evaluated the association between the MT1/MT2 expression ratio and patient 10-year survival using tumors expressing *MT1* and/or *MT2* (331 lower grade gliomas and 91 glioblastomas). Cutoffs used for patient dichotomization were defined using a log-rank test-based approach that identifies the most statistically significant data split, as previously described [36]. Univariate analyses of survival were performed using Kaplan-Meier curves and the log-rank test. Multivariate analyses of survival adjusting for clinically significant parameters were performed using Cox proportional hazards regression. Hazard ratios including 95% confidence intervals were calculated.

The Cancer Cell Line Encyclopedia (CCLE) data

RNA-seq and drug response data from 23 brain cancer cell lines expressing MT1 and/or MT2 were downloaded from the CCLE Depmap Portal (https://depmap.org/portal/)[37]. RNA-seq data were generated using the Illumina HiSeq 2000 RNA sequencing platform, quantified with RSEM, TPM-normalized and $\log_2(TPM + 1)$ transformed. Expression levels of *MT1* and *MT2* were converted to z-score for calculating the MT1/MT2 expression ratio. Drug response data were originally generated by the Broad Institute CTD2 Center (CTRP v2)[38] using CellTiter-Gl assays,

and represent the area under 16-point curves (AUC). We only considered compounds tested in at least 15 brain cancer cell lines.

RNA-seq

MGH143 and MGG23 cells (1,000 per well) were seeded in 96-well plates, left to rest overnight and treated with 5-HEAT (10^{-6} M) or vehicle (2 x 10^{-3} % DMSO) for 48 h. Culture media was removed after centrifugation and 10 μL of lysis buffer (SMART-Seq V4 Ultra Low Input RNA Kit; Clontech) was added to each well. Samples were incubated for 5 min at room temperature and transferred to −80°C. Once samples were thawed, reverse transcription and cDNA amplification (17 cycles) were performed with the SMART-Seq V4 Ultra Low Input RNA Kit according to the manufacturer's protocol. Following Agencourt Ampure XP beads cleanup (Beckman Coulter), 200 pg of amplified DNA were used for library preparation, as previously described[39]. Individual barcodes were ligated to each sample to allow multiplexing. Between 10 and 12 million single-end reads were sequenced per sample using an Illumina HiSeq 2500 v4 instrument. Reads were aligned to the GHCh38/hg38 human genome using Bowtie and expression values were quantified using RSEM. Data are presented as log2(TPM +1).

GSEA

For the TCGA RNA-seq data analysis, we selected tumors expressing MT1 and/or MT2 (331 lower grade gliomas and 91 glioblastomas), and used Pearson's correlation coefficient with the MT1/MT2 expression ratio as the ranking metric. For the glioma stem-like cells RNA-seq data analysis, genes were ranked according to the average log2(fold change) observed across samples treated with 5-HEAT compared to the vehicle group. GSEA was performed using the GSEA desktop application v3.0 [40] and Reactome pathways [41]. Enrichment scores (ES) were calculated based on a weighted Kolmogorov–Smirnov-like statistic and normalized (NES) to account for gene set size. P-values corresponding to each NES were calculated using 1,000 gene set permutations and corrected for multiple comparisons with the false discovery rate (FDR) procedure. Adjusted p-values < 0.1 were considered statistically significant. The Cytoscape plug-in EnrichmentMap was used to generate network-based enrichment maps of significantly enriched gene sets [42].

Additional statistical analysis

We used two-sided Student's t test or Wilcoxon test to perform two-group comparisons and Pearson's correlation to assess associations between continuous variable. Where specified, p values were corrected for multiple comparisons using the FDR procedure and combined using the Fisher's method. Sample size and number of experimental and technical replicates are reported in Figure Legends. P-values < 0.05 were considered statistically significant. Analyses were performed with GraphPad Prism 6 and R (www.r-project.org).

Results

Melatonin receptors MT1 and MT2 differentially control the proliferation of glioma and medulloblastoma cell lines

To explore the biological role of melatonin receptors in brain tumors, we first showed the expression of MT1 and MT2 in three human glioma cell lines (HOG, an oligodendroglioma grade III; T98G, a glioblastoma; and U87MG, a tumorigenic glioblastoma; **Fig. 1A**). The less aggressive cell lines HOG and T98G synthesize and accumulate significant amounts of melatonin in their microenvironment[12]. Using luzindole, a non-selective antagonist of melatonin receptors, we have previously demonstrated that this glioma-synthesized melatonin exerts an autocrine anti-proliferative effect in a receptor-dependent manner[12]. Thus, here, to elucidate the specific roles of MT1 and MT2, we treated cells with the MT2 antagonist DH97, which display 89-fold selectivity over MT1. Surprisingly, the selective blockage of MT2 by 10^{-8} M DH97 significantly decreased the proliferation of HOG and T98G (**Fig. 1B**). This effect was reverted, in a concentration dependent manner (DH97 10^{-7} – 10^{-6} M), by the concomitant inhibition of both melatonin receptors, suggesting opposite roles for MT1 and MT2 (**Fig. 1B**). Indeed, the treatment with 10^{-6} M DH97 mimicked the effects of the non-selective antagonist luzindole and stimulated the proliferation of HOG and T98G[12]. No difference was observed for the glioma cell line U87MG (**Fig. 1A**), which produces low levels of melatonin, and is also unaffected by luzindole[12]. We also analyzed the medulloblastoma cell line DAOY, which expresses MT1, MT2, and the enzymes involved in melatonin synthesis aralkylamine N-acetyltransferase (AANAT), its active form PAANAT, and ASMT (**Fig. S1A)**. DAOY accumulates significant amounts of melatonin (9.8 ±

0.7 pg/mL, n = 6, 6 h incubation) in the culture media and responded to DH97 with the same pattern observed in HOG and T98G (**Fig. S1B**). Interestingly, as previously described in gliomas[12], the levels of melatonin in the microenvironment of medulloblastomas, as predicted by the ASMT:CYP1B1 index, positively correlated with patient survival (**Fig. S1D**).

Clinical relevance of MT1 and MT2 expression in glioma

Analysis of TCGA and GTEx RNAseq data revealed that lower grade gliomas and glioblastomas have a decreased expression of *MT1* and an increased expression of *MT2* compared to normal brain cortex (**Fig. 2A)**, with similar results observed in medulloblastomas (**Fig. S1E**). Moreover, gliomas simultaneously expressing high *MT1* and low *MT2* (high MT1/MT2 ratio) were associated with significantly better 10-year survival **(Fig. 2B).** Such effect was especially relevant in gliomas predicted to synthesize and accumulate more melatonin, for which the MT1/MT2 ratio was a positive prognostic factor of 10-year survival independent of age, gender, IDH mutation and 1p/19q co-deletion (**Table 1**). Similar results were obtained for 5-year survival (**Table 2**). Next, in a way to assess whether a high MT1/MT2 ratio translates into enhanced MT1-induced Gq activation, using GSEA we showed that the ratio positively correlates with the expression of gene sets associated with calcium-dependent signaling (**Fig. 2C, Table S1**). In accordance with the *in vitro* results suggesting that MT1 has a negative, and MT2 a positive, impact on glioma growth, the MT1/MT2 ratio also negatively correlated with the expression of cell cycle-related gene sets (**Fig. 2C, 3A and Table S1**), while no significant results were observed for genes involved in apoptosis (**Fig. 3A and S2A**). Tumors with a high MT1/MT2 ratio presented a significantly decreased expression of cell cycle regulators such as the DNA replication factor PCNA, the cyclin CCNA2 and the cyclin-dependent kinases CDK2 (**Fig. 3A**). Accordingly, in CCLE brain cancer cell lines[37], the MT1/MT2 ratio negatively correlated with the sensitivity of these cells to inhibitors of cyclin-dependent kinases (**Fig. 3B-C**). Altogether, these results are highly consistent with the decreased proliferation associated with a high MT1/MT2 ratio.

Functional selective drugs that Simultaneously activate MT1 and inhibit MT2 exert robust anti-tumor effects

Given the opposite roles of melatonin receptors suggested by our data, we reasoned that drugs able to activate MT1 while inhibiting MT2 would have promising therapeutic potential. We

tested two high-affinity compounds that act as agonists of MT1 and antagonists of MT2: 5-HEAT, that bears an hydroxyethoxy group on the C5-indole position of melatonin[43], and UCM799, a N-anilinoethylamide derivative carrying a benzyl substituent on the aniline nitrogen[44]. 5-HEAT and UCM799 inhibited the *in vitro* proliferation of all four cell lines analyzed (HOG, T98G, U87MG, DAOY; **Fig. 4A-B, S1C**), including the low-melatonin cell line U87MG. The fact that the N-anilinoethylamide UCM799 reproduces the effect of the indoleamine 5-HEAT implies that the antioxidant activity ascribed to the indole ring of 5-HEAT plays a minor role in its tumor growth suppressive action. Next, we tested the therapeutic efficiency of such compounds *in vivo* using the U87MG-luc orthotopic xenograft model. We expect 5-HEAT and UCM799 to be effective regardless of the content of melatonin in the tumor microenvironment. For instance, given the limited capacity of U87MG cells to produce and accumulate melatonin, we postulate that *in vivo*, during the day, such compounds would act mainly by activating MT1, while at night they would also antagonize the binding of pineal melatonin to MT2. Notably, continuous brain infusion of 5-HEAT or UCM799 for 14 days reduced tumor growth by approximately 75% compared to vehicle (**Fig. 4C-D**), a robust therapeutic effect that likely reflects the complementary mechanisms of action of these functional selective drugs.

Cancer stem cells are a subpopulation within tumors that has enhanced tumorigenicity and is capable of self-renewal and differentiation[45]. In glioblastomas, the failure of current gold-standard therapies to eliminate tumor stem cells has been considered a major factor contributing to the inevitable tumor recurrence[46]. Thus, to better understand the mechanism of action of the functional selective melatonergic compounds, we used glioma stem cell-enriched neurosphere cultures MGG23 and MGH143, previously shown to maintain primary tumor phenotype and genotype[47,48]. Neurospheres were treated with vehicle or 5-HEAT 10^{-6} M for 48 h and profiled by RNA-seq. We then used GSEA to explore gene sets differentially expressed upon treatment in both cell lines. We identified 73 gene sets negatively enriched compared to the vehicle group, whereas no gene sets were positively enriched (**Fig. 5A, Table S2**). In both cell lines 5-HEAT inhibited the expression of cell cycle genes including CCND1, CDK4, CKD9, regulators of DNA replication RPA2, GINS2 and RFC2/5, as well as tubulins (**Fig. 5B, Table S3**). 5-HEAT also impaired the expression of multiple RNA processing and translation genes, and important regulators of cellular metabolism such as the glycolysis enzymes GAPDH and ENO1, translocases of inner mitochondrial membrane TOMM22, TIMM17B/22/50, and CYC1, which encodes a

subunit of the cytochrome bc1 complex, the third complex in the electron transport chain of the mitochondrial (**Fig. 5B, Table S3**). Importantly, the treatment of HOG, T98G, U87MG, MGG23 and MGH143 cells with 5-HEAT 10^{-6} M for 48h did not induce apoptosis/necrosis (**Fig. S2B-C**), reinforcing that its oncostatic effects mainly involve the impairment of cell cycle progression.

Discussion

The detailed characterization of the biological roles of melatonin receptors is essential for a rational clinical application of melatonin and other melatonergic compounds in the treatment of brain tumors. Despite the widespread interest in using melatonin as an adjuvant anticancer therapy, the specific effects mediated through the activation of MT1 and MT2 receptors remain poorly understood. Although accumulating studies support the anticancer properties of melatonin in different tumor types, experiments often involve millimolar concentrations of this indolamine[25], which likely trigger diverse receptor-independent mechanisms, masking the impact of MT1 and MT2 activation. In this respect, here we demonstrated that, in glioma and medulloblastoma, the receptor-dependent anti-proliferative effect of melatonin is mediated by the activation of MT1, whereas MT2 seems to play an pro-tumor role and has a significantly higher mRNA expression in tumors compared to the normal brain cortex. Accordingly, the ratio between the expression of MT1 and MT2 is a positive prognostic factor of patient survival, being particularly relevant when considering tumors with higher local production and accumulation of melatonin. Finally, we also showed the potential of MT1 and MT2 receptors as druggable targets, as the simultaneous activation of MT1 and inhibition of MT2 promotes a decrease in the expression of genes related to cell cycle, metabolism and protein translation in glioma stem-like cells, besides impairing tumor growth *in vitro* and *in vivo*.

MT1 has often been recognized as the mediator of receptor-dependent antitumor actions of melatonin[25]. Studies with melanoma and breast cancer cell lines demonstrated that MT1 overexpression potentiates the growth suppressive effects of melatonin[49–51]. In estrogen receptor positive ductal breast carcinomas, MT1 protein levels decrease with tumor grade and positively correlates with patient overall survival[52]. Moreover, mRNA expression of *MT1* is significant decreased in colorectal cancer compared to the adjacent mucosa[53]. In contrast, activation of

MT2 receptors in the brain has been linked to the neuroprotection conferred by melatonin following ischemic strokes[54,55]. Treatment with melatonin enhances endogenous neurogenesis and cell proliferation in the peri-infarct regions in a MT2-dependent manner, improving survival rates and the neural functioning of mice[54]. Under high glucose conditions, melatonin has also been shown to prevent neuronal cell apoptosis via a MT2/Akt/NF-κB pathway[56]. Importantly, in Alzheimer's disease patients, the hippocampal expression of MT1 is upregulated and of MT2 is downregulated [23,24]. Moreover, MT2 activation prevents the disruption of dendritic complexity and spine induced by amyloid β in hippocampal neuron cultures[57]. Altogether, these findings corroborate the idea that MT1 and MT2 have opposite roles controlling cell proliferation in the brain, a pattern that seems to be preserved in brain cancer cells, as revealed by our data.

Recent studies using subtype selective receptor ligands and knockout mice suggest that MT1 and MT2 also play differential roles in process such as the control of sleep and body temperature[58,59]. Activation of MT1 receptors seems to be implicated in the regulation of rapid eye movement (REM) sleep, whereas MT2 receptors selectively increase non-REM (NREM) sleep[58]. MT1 knockout mice have an increase in NREM sleep and a decrease in REM sleep, while MT2 knockout mice have a decrease in NREM sleep. Regarding thermal regulation, administration of the MT1-selective partial agonist UCM871 and the MT2-selective partial agonist UCM924 have been shown to impact body temperature at different times of the dark phase and with opposite magnitude. UCM871 enhances body temperature just after the light–dark transition, whereas UCM924 decreases body temperature just before the dark–light transition[59].

The current mainstay treatment of glioblastomas (i.e. maximal surgical resection, concurrent chemoradiation and adjuvant chemotherapy) offers only palliation and is normally followed by tumor recurrence[60]. In this regard, the clinical significance of glioma stem cells is supported by studies showing their ability to promote radioresistance by preferential activation of the DNA damage responses[61], and to propagate tumor growth after chemotherapy[62]. Single-cell RNA-seq characterization of different types of glioma, including glioblastomas, has also shown that cycling cells within human tumors are enriched in stem-like subpopulation[47,63,64]. Notably, the MT1 agonist and MT2 antagonist 5-HEAT suppressed the expression of multiple cell cycle and translation related genes in stem cell-enriched cultures, as well as seemed to interfere with their energy metabolism; mechanisms that likely contribute the robust growth suppressive effect of 5-HEAT observed *in vivo.* Additionally, the ability of 5-HEAT to downregulate the expression of

both glycolysis enzymes and mitochondrial proteins might be specially beneficial given the capacity of glioblastoma stem cells to rely on both oxidative and non-oxidative glucose metabolism, depending on the environment conditions[65,66].

Overall, here we provided the first evidences regarding the differential role of MT1 and MT2 in brain tumor progression, supporting further investigations of their specific signaling pathways[67]. Our findings suggest that melatonin antitumor effects mediated by MT1 can be counterbalanced by the pro-tumor MT2 activation, what could be especially relevant in tumors expressing low MT1 and high MT2. More importantly, we highlight the clinical potential of selective melatonergic compounds, 5-HEAT and UCM799, that activate MT1 and/or inhibit MT2 receptors in brain cancer therapy. Both compounds might be of particular clinical interest as their amphiphilic molecular structure[43,44] allows them to cross the blood brain barrier and penetrate the central nervous system following systemic administration, overcoming the drug delivery challenge that is often faced in neuropharmacology.

Author contributions

G.S.K, L.H.O, S.M.M., T.G.S., R.P.M, and P.A.F. designed the study. G.S.K., L.H.O., P.A.C.R. and R.C. performed the experiments. S.M.M., I.T., S.R., V.R.M, T.G.S, R.P.M, P.A.F contributed with reagents, material, and analysis tools. G.S.K, L.H.O., R.P.M and P.A.F analyzed the data and G.S.K wrote the manuscript. All authors critically revised the manuscript and approved the final version to be published. R.P.M and P.A.F supervised the project.

Conflict of interest

The authors declare no conflict of interest.

Acknowledgements

The authors gratefully thank D. A. Moura for the technical support.

Funding

This work was supported by funds from the Sao Paulo Research Foundation (FAPESP) to G.S.K (14/27287-0 and 17/24287-8, fellowships), L.H.O (14/23830-1, fellowship), R.P.M. (13/13691-1, Grant) and P.A.F. (15/23348-8, Grant), and by the National Institutes of Science and Technology

(INCTs) Program (V.R.M, 14/50943-1, Grant) from FAPESP, the National Council for Scientific and Technological Development (CNPq) and the Coordination for the Improvement of Higher Education Personnel (CAPES).

Ethical approval

All procedures performed in experiments involving animals were approved by the Animal Ethics Committee of the A. C. Camargo Cancer Center (ID 076/17), and by the Animal Ethics Committee of the Institute of Bioscience of the University of Sao Paulo (ID 284/2017).

Consent to participate

Not applicable.

Consent for publication

Not applicable.

Availability of data and materials

Not applicable.

References

1. Chinot OL, Wick W, Mason W, et al. Bevacizumab plus Radiotherapy–Temozolomide for Newly Diagnosed Glioblastoma. *N Engl J Med*. 2014;370(8):709-722. doi:10.1056/NEJMoa1308345
2. Gilbert MR, Dignam JJ, Armstrong TS, et al. A Randomized Trial of Bevacizumab for Newly Diagnosed Glioblastoma. *N Engl J Med*. 2014;370(8):699-708. doi:10.1056/NEJMoa1308573
3. Aldape K, Brindle KM, Chesler L, et al. Challenges to curing primary brain tumours. *Nat Rev Clin Oncol*. 2019;16(8):509-520. doi:10.1038/s41571-019-0177-5
4. Louis DN, Perry A, Reifenberger G, et al. The 2016 World Health Organization Classification of Tumors of the Central Nervous System: a summary. *Acta Neuropathol*. 2016;131(6):803-820. doi:10.1007/s00401-016-1545-1
5. Reifenberger G, Wirsching H-G, Knobbe-Thomsen CB, Weller M. Advances in the molecular genetics of gliomas — implications for classification and therapy. *Nat Rev Clin Oncol*. 2017;14(7):434-452. doi:10.1038/nrclinonc.2016.204
6. Hardeland R, Madrid JA, Tan D-X, Reiter RJ. Melatonin, the circadian multioscillator system and health: the need for detailed analyses of peripheral melatonin signaling. *J*

Pineal Res. 2012;52(2):139-166. doi:10.1111/j.1600-079X.2011.00934.x
7. Reiter RJ. The melatonin rhythm: both a clock and a calendar. *Experientia*. 1993;49(8):654-664. doi:10.1007/BF01923947
8. Tosini G, Menaker M. Circadian rhythms in cultured mammalian retina. *Science*. 1996;272(5260):419-421. doi:10.1126/science.272.5260.419
9. Bubenik GA, Brown GM. Pinealectomy Reduces Melatonin Levels in the Serum but Not in the Gastrointestinal Tract of Rats. *Neurosignals*. 1997;6(1):40-44. doi:10.1159/000109107
10. Golan K, Kumari A, Kollet O, et al. Daily Onset of Light and Darkness Differentially Controls Hematopoietic Stem Cell Differentiation and Maintenance. *Cell Stem Cell*. 2018;23(4):572-585.e7. doi:10.1016/J.STEM.2018.08.002
11. Córdoba-Moreno MO, de Souza E da S, Quiles CL, et al. Rhythmic expression of the melatonergic biosynthetic pathway and its differential modulation in vitro by LPS and IL10 in bone marrow and spleen. *Sci Rep*. 2020;10(1):4799. doi:10.1038/s41598-020-61652-5
12. Kinker GS, Oba-Shinjo SM, Carvalho-Sousa CE, et al. Melatonergic system-based two-gene index is prognostic in human gliomas. *J Pineal Res*. 2016;60(1):84-94. doi:10.1111/jpi.12293
13. Pinato L, da Silveira Cruz-Machado S, Franco DG, et al. Selective protection of the cerebellum against intracerebroventricular LPS is mediated by local melatonin synthesis. *Brain Struct Funct.* 2015;220(2):827-840. doi:10.1007/s00429-013-0686-4
14. Bubenik GA. REVIEW: Gastrointestinal Melatonin: Localization, Function, and Clinical Relevance. *Dig Dis Sci*. 2002;47(10):2336-2348. doi:10.1023/A:1020107915919
15. Venegas C, García JA, Escames G, et al. Extrapineal melatonin: analysis of its subcellular distribution and daily fluctuations. *J Pineal Res*. 2012;52(2):217-227. doi:10.1111/j.1600-079X.2011.00931.x
16. Tan D, Reiter R, Manchester L, et al. Chemical and Physical Properties and Potential Mechanisms: Melatonin as a Broad Spectrum Antioxidant and Free Radical Scavenger. *Curr Top Med Chem*. 2002;2(2):181-197. doi:10.2174/1568026023394443
17. Reppart SM, Weaver DR, Godson C. Melatonin receptors step into the light: cloning and classification of subtypes. *Trends Pharmacol Sci*. 1996;17(3):100-102. doi:10.1016/0165-6147(96)10005-5
18. Brydon L, Roka F, Petit L, et al. Dual Signaling of Human Mel1a Melatonin Receptors via G_{i2} , G_{i3} , and $G_{q/11}$ Proteins. *Mol Endocrinol*. 1999;13(12):2025-2038. doi:10.1210/mend.13.12.0390
19. Jockers R, Delagrange P, Dubocovich ML, et al. Update on melatonin receptors: IUPHAR Review 20. *Br J Pharmacol*. 2016;173(18):2702-2725. doi:10.1111/bph.13536
20. Klosen P, Lapmanee S, Schuster C, et al. MT1 and MT2 melatonin receptors are expressed in nonoverlapping neuronal populations. *J Pineal Res*. 2019;67(1):e12575. doi:10.1111/jpi.12575
21. Ng KY, Leong MK, Liang H, Paxinos G. Melatonin receptors: distribution in mammalian brain and their respective putative functions. *Brain Struct Funct*. 2017;222(7):2921-2939. doi:10.1007/s00429-017-1439-6
22. Adi N, Mash DC, Ali Y, Singer C, Shehadeh L, Papapetropoulos S. Melatonin MT1 and MT2 receptor expression in Parkinson's disease. *Med Sci Monit*. 2010;16(2):61-67.
23. Savaskan E, Olivieri G, Meier F, et al. Increased melatonin 1a-receptor immunoreactivity

in the hippocampus of Alzheimer's disease patients. *J Pineal Res*. 2002;32(1):59-62. doi:10.1034/j.1600-079x.2002.00841.x
24. Savaskan E, Ayoub MA, Ravid R, et al. Reduced hippocampal MT2 melatonin receptor expression in Alzheimer's disease. *J Pineal Res*. 2005;38(1):10-16. doi:10.1111/j.1600-079X.2004.00169.x
25. Li Y, Li S, Zhou Y, et al. Melatonin for the prevention and treatment of cancer. *Oncotarget*. 2017;8(24):39896-39921. doi:10.18632/oncotarget.16379
26. Cutando A, López-Valverde A, Arias-Santiago S, DE Vicente J, DE Diego RG. Role of melatonin in cancer treatment. *Anticancer Res*. 2012;32(7):2747-2753. http://www.ncbi.nlm.nih.gov/pubmed/22753734. Accessed September 8, 2019.
27. Martín V, Sanchez-Sanchez AM, Puente-Moncada N, et al. Involvement of autophagy in melatonin-induced cytotoxicity in glioma-initiating cells. *J Pineal Res*. 2014;57(3):308-316. doi:10.1111/jpi.12170
28. Wang J, Hao H, Yao L, et al. Melatonin suppresses migration and invasion via inhibition of oxidative stress pathway in glioma cells. *J Pineal Res*. 2012;53(2):180-187. doi:10.1111/j.1600-079X.2012.00985.x
29. Zheng X, Pang B, Gu G, et al. Melatonin Inhibits Glioblastoma Stem-like cells through Suppression of EZH2-NOTCH1 Signaling Axis. *Int J Biol Sci*. 2017;13(2):245-253. doi:10.7150/ijbs.16818
30. Lee H, Lee H-J, Jung JH, Shin EA, Kim S-H. Melatonin disturbs SUMOylation-mediated crosstalk between c-Myc and nestin via MT1 activation and promotes the sensitivity of paclitaxel in brain cancer stem cells. *J Pineal Res*. 2018;65(2):e12496. doi:10.1111/jpi.12496
31. Ma H, Wang Z, Hu L, et al. The melatonin-MT1 receptor axis modulates tumor growth in PTEN-mutated gliomas. *Biochem Biophys Res Commun*. 2018;496(4):1322-1330. doi:10.1016/J.BBRC.2018.02.010
32. Lopes MH, Santos TG, Rodrigues BR, et al. Disruption of prion protein–HOP engagement impairs glioblastoma growth and cognitive decline and improves overall survival. *Oncogene*. 2015;34(25):3305-3314. doi:10.1038/onc.2014.261
33. Wasilewska-Sampaio AP, Santos TG, Lopes MH, Cammarota M, Martins VR. The growth of glioblastoma orthotopic xenografts in nude mice is directly correlated with impaired object recognition memory. *Physiol Behav*. 2014;123:55-61. doi:10.1016/J.PHYSBEH.2013.09.012
34. Marianecci C, Rinaldi F, Hanieh PN, Di Marzio L, Paolino D, Carafa M. Drug delivery in overcoming the blood-brain barrier: role of nasal mucosal grafting. *Drug Des Devel Ther*. 2017;11:325-335. doi:10.2147/DDDT.S100075
35. Goldman M, Craft B, Kamath A, Brooks A, Zhu J, Haussler D. The UCSC Xena Platform for cancer genomics data visualization and interpretation. *bioRxiv*. August 2018:326470. doi:10.1101/326470
36. Budczies J, Klauschen F, Sinn B V, et al. Cutoff Finder: a comprehensive and straightforward Web application enabling rapid biomarker cutoff optimization. *PLoS One*. 2012;7(12):e51862. doi:10.1371/journal.pone.0051862
37. Ghandi M, Huang FW, Jané-Valbuena J, et al. Next-generation characterization of the Cancer Cell Line Encyclopedia. *Nature*. 2019;569(7757):503-508. doi:10.1038/s41586-019-1186-3
38. Viswanathan VS, Ryan MJ, Dhruv HD, et al. Dependency of a therapy-resistant state of

cancer cells on a lipid peroxidase pathway. *Nature*. 2017;547(7664):453-457. doi:10.1038/nature23007
39. Blecher-Gonen R, Barnett-Itzhaki Z, Jaitin D, Amann-Zalcenstein D, Lara-Astiaso D, Amit I. High-throughput chromatin immunoprecipitation for genome-wide mapping of in vivo protein-DNA interactions and epigenomic states. *Nat Protoc*. 2013;8(3):539-554. doi:10.1038/nprot.2013.023
40. Subramanian A, Tamayo P, Mootha VK, et al. Gene set enrichment analysis: a knowledge-based approach for interpreting genome-wide expression profiles. *Proc Natl Acad Sci U S A*. 2005;102(43):15545-15550. doi:10.1073/pnas.0506580102
41. Fabregat A, Sidiropoulos K, Garapati P, et al. The Reactome pathway Knowledgebase. *Nucleic Acids Res*. 2016;44(D1):D481-D487. doi:10.1093/nar/gkv1351
42. Merico D, Isserlin R, Stueker O, Emili A, Bader GD. Enrichment Map: A Network-Based Method for Gene-Set Enrichment Visualization and Interpretation. *PLoS One*. 2010;5(11). doi:10.1371/JOURNAL.PONE.0013984
43. Nonno R, Lucini V, Spadoni G, et al. A new melatonin receptor ligand with mt1-agonist and MT2-antagonist properties. *J Pineal Res*. 2000;29(4):234-240. doi:10.1034/j.1600-0633.2002.290406.x
44. Rivara S, Lodola A, Mor M, et al. *N* -(Substituted-anilinoethyl)amides: Design, Synthesis, and Pharmacological Characterization of a New Class of Melatonin Receptor Ligands. *J Med Chem*. 2007;50(26):6618-6626. doi:10.1021/jm700957j
45. Batlle E, Clevers H. Cancer stem cells revisited. *Nat Med*. 2017;23(10):1124-1134. doi:10.1038/nm.4409
46. Lathia JD, Mack SC, Mulkearns-Hubert EE, Valentim CLL, Rich JN. Cancer stem cells in glioblastoma. *Genes Dev*. 2015;29(12):1203-1217. doi:10.1101/gad.261982.115
47. Neftel C, Laffy J, Filbin MG, et al. An Integrative Model of Cellular States, Plasticity, and Genetics for Glioblastoma. *Cell*. 2019;178(4):835-849.e21. doi:10.1016/J.CELL.2019.06.024
48. Wakimoto H, Mohapatra G, Kanai R, et al. Maintenance of primary tumor phenotype and genotype in glioblastoma stem cells. *Neuro Oncol*. 2012;14(2):132-144. doi:10.1093/neuonc/nor195
49. Collins A, Yuan L, Kiefer TL, Cheng Q, Lai L, Hill SM. Overexpression of the MT1 melatonin receptor in MCF-7 human breast cancer cells inhibits mammary tumor formation in nude mice. *Cancer Lett*. 2003;189(1):49-57. doi:10.1016/S0304-3835(02)00502-5
50. Kadekaro AL, Andrade LNS, Floeter-Winter LM, et al. MT-1 melatonin receptor expression increases the antiproliferative effect of melatonin on S-91 murine melanoma cells. *J Pineal Res*. 2004;36(3):204-211. doi:10.1111/j.1600-079X.2004.00119.x
51. Yuan L, Collins AR, Dai J, Dubocovich ML, Hill SM. MT1 melatonin receptor overexpression enhances the growth suppressive effect of melatonin in human breast cancer cells. *Mol Cell Endocrinol*. 2002;192(1-2):147-156. doi:10.1016/S0303-7207(02)00029-1
52. Jablonska K, Pula B, Zemla A, et al. Expression of melatonin receptor MT1 in cells of human invasive ductal breast carcinoma. *J Pineal Res*. 2013;54(3):334-345. doi:10.1111/jpi.12032
53. Nemeth C, Humpeler S, Kallay E, et al. Decreased expression of the melatonin receptor 1 in human colorectal adenocarcinomas. *J Biol Regul Homeost Agents*. 2011;25(4):531-542.

http://www.ncbi.nlm.nih.gov/pubmed/22217986. Accessed July 24, 2019.
54. Chern C-M, Liao J-F, Wang Y-H, Shen Y-C. Melatonin ameliorates neural function by promoting endogenous neurogenesis through the MT2 melatonin receptor in ischemic-stroke mice. *Free Radic Biol Med*. 2012;52(9):1634-1647. doi:10.1016/J.FREERADBIOMED.2012.01.030
55. Lee CH, Yoo K-Y, Choi JH, et al. Melatonin's protective action against ischemic neuronal damage is associated with up-regulation of the MT2 melatonin receptor. *J Neurosci Res*. 2010;88(12):n/a-n/a. doi:10.1002/jnr.22430
56. Onphachanh X, Lee HJ, Lim JR, et al. Enhancement of high glucose-induced PINK1 expression by melatonin stimulates neuronal cell survival: Involvement of MT 2 /Akt/NF-κB pathway. *J Pineal Res*. 2017;63(2):e12427. doi:10.1111/jpi.12427
57. Tang H, Ma M, Wu Y, et al. Activation of MT2 receptor ameliorates dendritic abnormalities in Alzheimer's disease via C/EBPα/miR-125b pathway. *Aging Cell*. 2019;18(2):e12902. doi:10.1111/acel.12902
58. Gobbi G, Comai S. Differential Function of Melatonin MT1 and MT2 Receptors in REM and NREM Sleep. *Front Endocrinol (Lausanne)*. 2019;10:87. doi:10.3389/fendo.2019.00087
59. López-Canul M, Min SH, Posa L, et al. Melatonin MT1 and MT2 Receptors Exhibit Distinct Effects in the Modulation of Body Temperature across the Light/Dark Cycle. *Int J Mol Sci*. 2019;20(10):2452. doi:10.3390/ijms20102452
60. Stupp R, Hegi ME, Mason WP, et al. Effects of radiotherapy with concomitant and adjuvant temozolomide versus radiotherapy alone on survival in glioblastoma in a randomised phase III study: 5-year analysis of the EORTC-NCIC trial. *Lancet Oncol*. 2009;10(5):459-466. doi:10.1016/S1470-2045(09)70025-7
61. Bao S, Wu Q, McLendon RE, et al. Glioma stem cells promote radioresistance by preferential activation of the DNA damage response. *Nature*. 2006;444(7120):756-760. doi:10.1038/nature05236
62. Chen J, Li Y, Yu T-S, et al. A restricted cell population propagates glioblastoma growth after chemotherapy. *Nature*. 2012;488(7412):522-526. doi:10.1038/nature11287
63. Filbin MG, Tirosh I, Hovestadt V, et al. Developmental and oncogenic programs in H3K27M gliomas dissected by single-cell RNA-seq. *Science (80-)*. 2018;360(6386):331-335. doi:10.1126/science.aao4750
64. Tirosh I, Venteicher AS, Hebert C, et al. Single-cell RNA-seq supports a developmental hierarchy in human oligodendroglioma. *Nature*. 2016;539(7628):309-313. doi:10.1038/nature20123
65. Vlashi E, Lagadec C, Vergnes L, et al. Metabolic state of glioma stem cells and nontumorigenic cells. *Proc Natl Acad Sci U S A*. 2011;108(38):16062-16067. doi:10.1073/pnas.1106704108
66. Marin-Valencia I, Yang C, Mashimo T, et al. Analysis of Tumor Metabolism Reveals Mitochondrial Glucose Oxidation in Genetically Diverse Human Glioblastomas in the Mouse Brain In Vivo. *Cell Metab*. 2012;15(6):827-837. doi:10.1016/j.cmet.2012.05.001
67. Ayoub MA, Couturier C, Lucas-Meunier E, et al. Monitoring of ligand-independent dimerization and ligand-induced conformational changes of melatonin receptors in living cells by bioluminescence resonance energy transfer. *J Biol Chem*. 2002;277(24):21522-21528. doi:10.1074/jbc.M200729200

Figures and legends

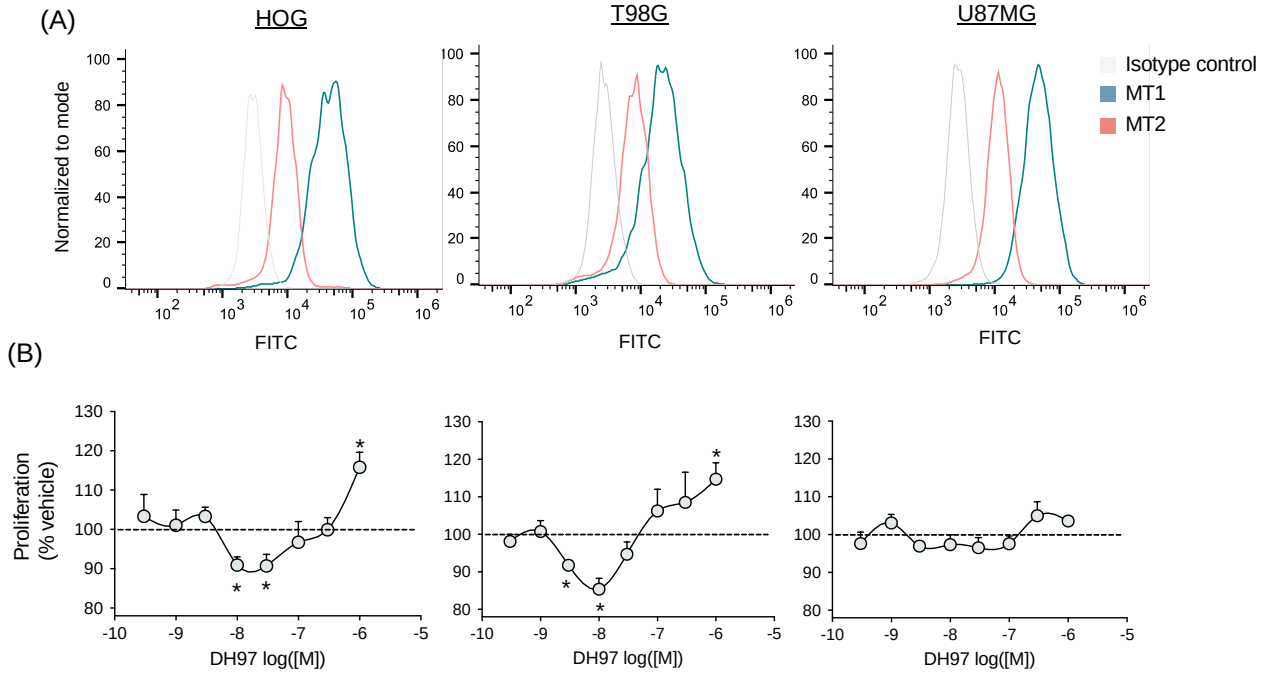

Figure 1. Activation of MT1 and MT2 receptors plays opposite roles in the control of glioma proliferation. (A) Detection of melatonin receptors by indirect immunofluorescence using flow cytometry. Isotype control corresponds to cells stained with secondary antibody alone. **(B)** High- (HOG and T98G) and low-melatonin (U87MG) glioma cell lines were cultured for 48 h in the presence of DH97 (3×10^{-10} – 10^{-6} M), an MT2-selective antagonist (pKi = 8.03, 89-fold selectivity over MT1), or the respective vehicle (7×10^{-7} – 2×10^{-3} % DMSO). Cell number was estimated by MTT assay and values were normalized by the mean absorbance detected in the respective vehicle group. Data are shown as mean ± SEM of four independent experiments in quadruplicates. * Significantly different from the respective vehicle group ($p < 0.05$) using two-sided Student's t test.

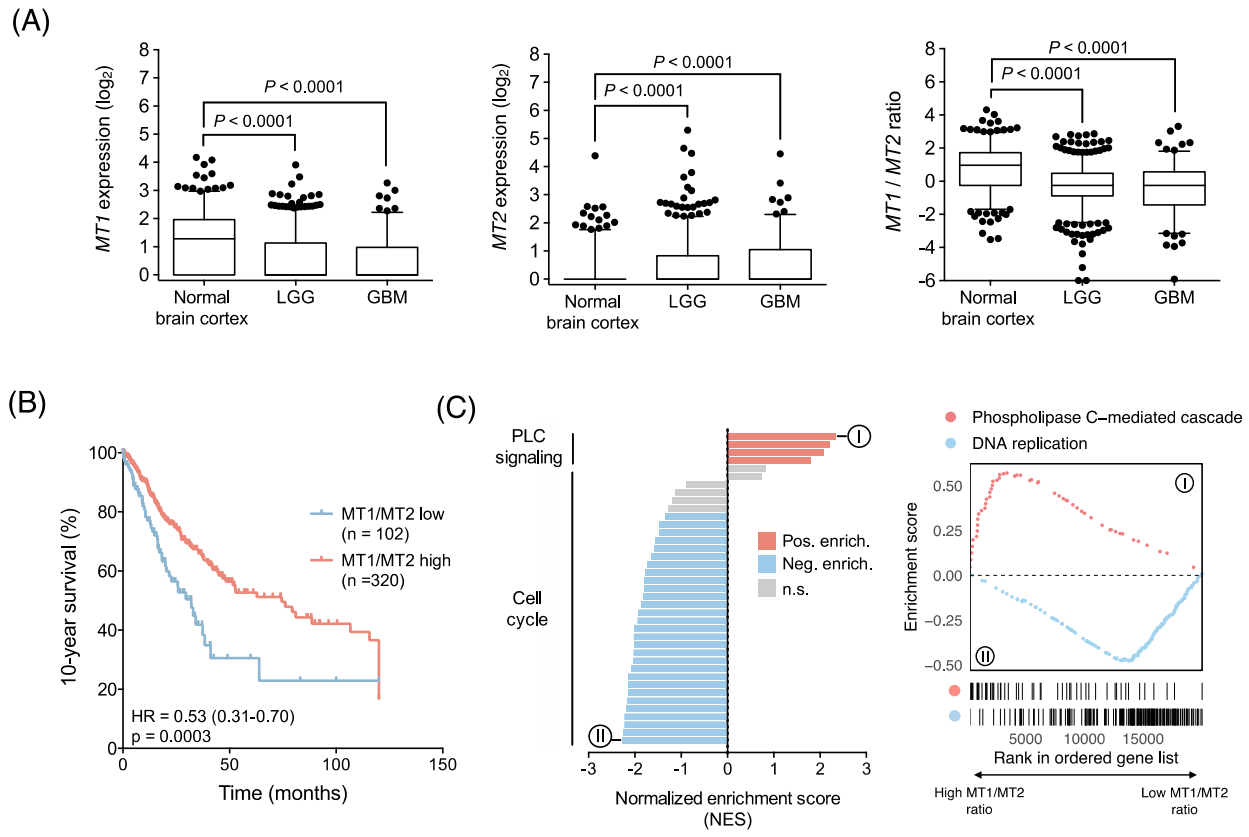

Figure 2. Expression of *MT1* and *MT2* differentially impact glioma patient survival. (A) Expression of *MT1* and *MT2* and the MT1/MT2 ratio in normal brain cortexes (n = 283) from GTEx and primary lower grade gliomas (LGG, n = 509) and glioblastomas (GBM, n = 153) from TCGA. Boxes extend from the 25th to the 75th percentile, the central bold line shows the median, and whiskers are drawn from the 5th to the 95th percentile. Samples below and above the whiskers are shown as individual points. Comparisons were performed using two-sided Wilcoxon test. **(B)** Kaplan-Meier survival curves of gliomas patients with high vs. low MT1/MT2 expression ratios. Comparisons were performed using the log-rank test. **(C)** Gene set enrichment analysis testing the correlation between the MT1/MT2 expression ratio and the expression of genes related to the cell cycle and phospholipase C signaling in gliomas. Bar plots show normalized enrichment scores of the Reactome gene sets analyzed. FDR adjusted p values < 0.1 were considered statistically significant.

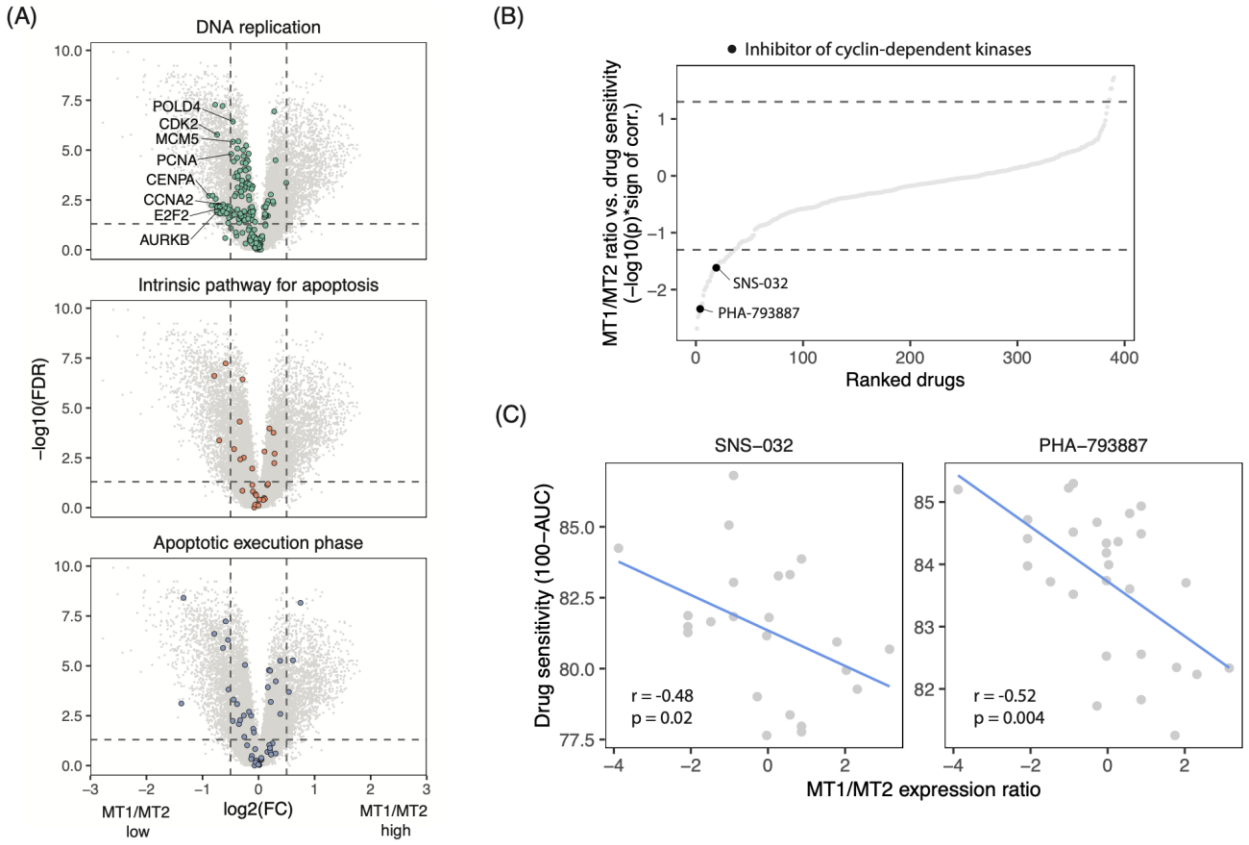

Figure 3. A high MT1/MT2 expression ration is associated with decreased expression of cell cycle genes in human glioma samples. (A) Volcano plot showing differential expression analysis comparing tumors with high vs. low MT1/MT2 expression ratios, as in **Fig. 2B**. P values were calculated using two-sided Student's t test and FDR-adjusted. Dashed lines denote an FDR value of 0.05 and a $\log_2$(fold change) of 0.5 and -0.5. Reactome gene sets related to cell cycle and apoptosis are marked in different colors. Relevant genes are annotated. **(B)** Pearson's correlation between drug response (CTRPv2 database) and the MT1/MT2 expression ratio in brain cancer cell lines. Drugs are ranked from lowest to highest correlation. Dashed lines denote a p value threshold of 0.05. Inhibitors of cyclin-dependent kinases are highlighted. **(C)** Scatterplots depicts the negative correlation between the MT1/MT2 expression ratio and the sensitivity to inhibitors of cyclin-dependent kinases.

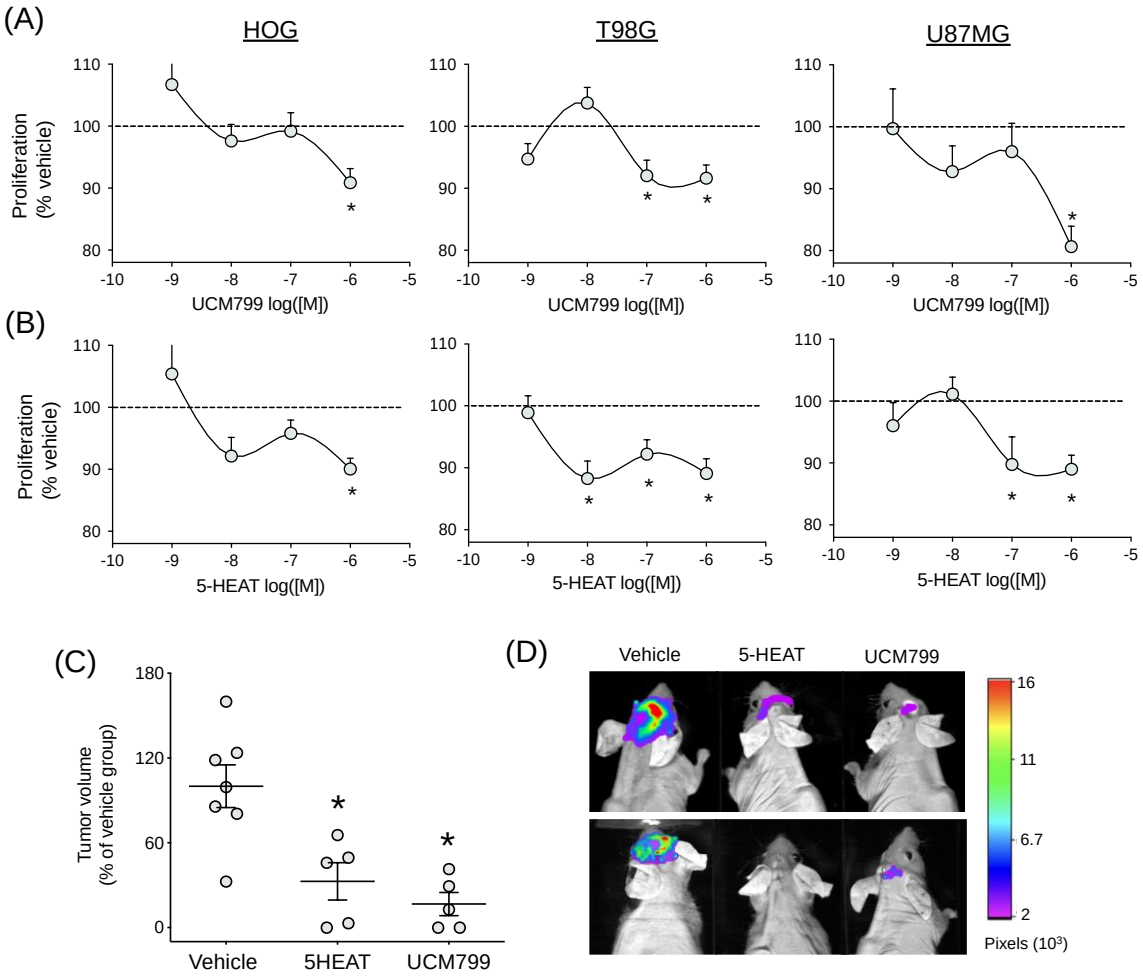

Figure 4. The simultaneous activation of MT1 and inhibition of MT2 by functional-selective drugs impairs glioma growth in vitro and in vivo. (A)-(B) High- (HOG and T98G) and low-melatonin (U87MG) glioma cell lines were cultured for 48 h with drugs that simultaneously activate MT1 and inhibit MT2, 5-HEAT and UCM799 (10^{-9} – 10^{-6} M), or the respective vehicle (2 x 10^{-6} – 2 x 10^{-3} % DMSO). Cell number was estimated by MTT assay and values were normalized by the mean absorbance detected in the respective vehicle group. Data are shown as mean ± SEM of four independent experiments in quadruplicates. **(C)** Mice with pre-stablished U87MG-luc orthotopic tumors received continuous brain infusions of vehicle (0.2% DMSO), 10^{-4} M 5-HEAT or 10^{-4} M UCM799. Mice were euthanized 14 days after treatment initiation for tumor volume evaluation. Values were normalized by the average tumor volume of the vehicle group. Data are shown as mean ± SEM of five independent experiments. **(D)** *In vivo* bioluminescence imaging of tumor burden 14 days post-treatment. * Significantly different from the respective vehicle group ($p < 0.05$) using two-sided Student's t test.

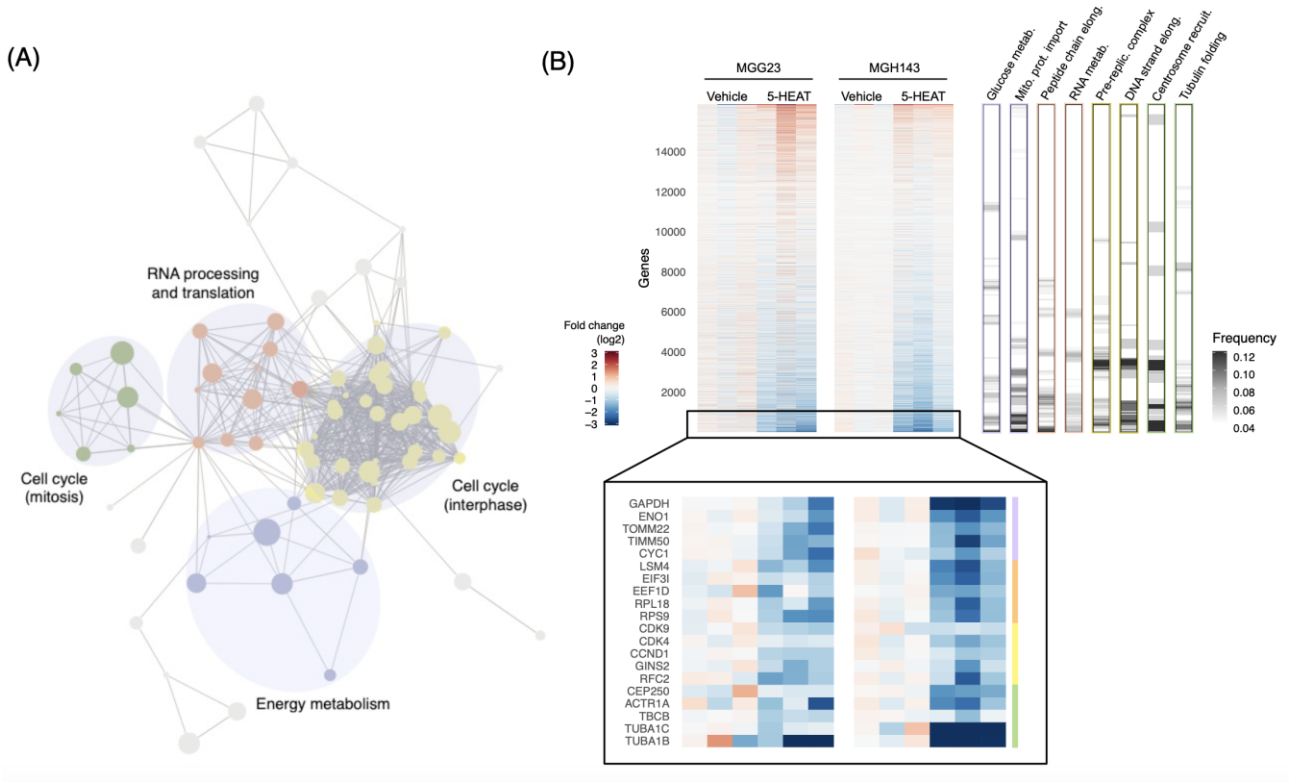

Figure 5. Impact of 5-HEAT on the expression profile of glioma stem-like cells. (A) MGG23 and MGH143 stem cell-enriched neurosphere cultures were incubated with 10^{-6} M 5-HEAT or vehicle (2 x 10^{-3} % DMSO) for 48 h and profiled by RNA-seq. Reactome gene sets differentially expressed in 5-HEAT treated cells compared to vehicle were identified using GSEA. Enrichment map shows negatively enriched gene sets (FDR adjusted $p < 0.1$) composing 4 main modules. Each gene set is a node and edges represent the similarity between gene sets. Node size shows enrichment significance (-log10(FDR-adjusted p)) and edge thickness is proportional to the overlap coefficient between gene sets. **(B)** Heatmap depicts the expression profile of 5-HEAT treated cells. Genes are ranked according to their average log2(expression fold change) in the 5-HEAT group compared to the vehicle. Bars on the right show the frequency of genes from selected gene sets within sliding windows of 500 genes. Relevant genes from each of the four gene set modules are highlighted in the bottom. Data correspond to three independent experiments.

Tables

Table 1. Multivariate Cox analysis of 10-year survival in gliomas.

	10-year survival							
	Low melatonin gliomas*				High melatonin gliomas*			
	Univariate		Multivariate		Univariate		Multivariate	
Variable	**HR (95% CI)**	**P value**	**HR (95% CI)**	**P value**	**HR (95% CI)**	**P value**	**HR (95% CI)**	**P value**
Gender (male vs. female)	0.79 (0.52-1.22)	0.297	1 (0.64-1.56)	0.984	1.75 (1.06-2.9)	0.03	1.46 (0.87-2.45)	0.156
Age	1.07 (1.05-1.09)	<0.001	1.05 (1.03-1.06)	<0.001	1.07 (1.05-1.09)	<0.001	1.04 (1.02-1.06)	<0.001
IDH mutation (yes vs. no)	0.12 (0.07-0.2)	<0.001	0.16 (0.08-0.32)	<0.001	0.15 (0.09-0.25)	<0.001	0.32 (0.16-0.64)	0.001
1p/19q codel (yes vs. no)	0.29 (0.14-0.6)	0.001	0.62 (0.26-1.49)	0.285	0.21 (0.09-0.49)	<0.001	0.38 (0.15-0.97)	0.043
MT1/MT2 ratio (high vs. low)	0.61 (0.38-0.97)	0.035	1.03 (0.63-1.69)	0.897	0.48 (0.27-0.86)	0.013	0.48 (0.27-0.87)	0.015

HR: hazard ratio. CI: confidence interval

*As predicted by the ASMY:CYP1B1 index

Table 2. Multivariate Cox analysis of 5-year survival in gliomas.

	5-year survival							
	Low melatonin gliomas*				High melatonin gliomas*			
	Univariate		Multivariate		Univariate		Multivariate	
Variable	**HR (95% CI)**	**P value**	**HR (95% CI)**	**P value**	**HR (95% CI)**	**P value**	**HR (95% CI)**	**P value**
Gender (male vs. female)	0.82 (0.52-1.3)	0.397	0.97 (0.6-1.55)	0.889	1.78 (1.05-3.04)	0.033	1.4 (0.81-2.41)	0.232
Age	1.07 (1.05-1.09)	<0.001	1.05 (1.03-1.07)	<0.001	1.07 (1.05-1.09)	<0.001	1.04 (1.02-1.07)	<0.001
IDH mutation (yes vs. no)	0.08 (0.05-0.15)	<0.001	0.23 (0.11-0.46)	<0.001	0.13 (0.08-0.23)	<0.001	0.34 (0.16-0.72)	0.005
1p/19q codel (yes vs. no)	0.16 (0.06-0.43)	<0.001	0.28 (0.09-0.88)	0.029	0.16 (0.06-0.45)	<0.001	0.34 (0.11-1.02)	0.054
MT1/MT2 ratio (high vs. low)	0.56 (0.35-0.91)	**0.019**	0.83 (0.51-1.36)	0.459	0.48 (0.27-0.86)	**0.013**	0.49 (0.27-0.88)	**0.017**

HR: hazard ratio. CI: confidence interval

*As predicted by the ASMY:CYP1B1 index